SPECTROMETER DESIGN AT LASL*

Henry A. Thiessen and Morris M. Klein
Los Alamos Scientific Laboratory
University of California
Los Alamos, New Mexico

Abstract

We review the results of recent work at Los Alamos in the area of spectrometer design. Included are reports of results of bending magnet design using H_t-windings for fine adjustment of the field uniformity, high quality quadrupole design, and high resolution detectors. We discuss details of an optimizing ray tracing program called MOTER, and give serveral recent results obtained with this program. We believe that the techniques reported here represent significant developments in the technology of spectrometer design and have important applications in the areas of medium energy and high energy physics.

I. Introduction

We review recent developments in the area of spectrometer design at LASL and present a collection of the highlights of new techniques and results which may be of interest. Complete reports will be published at a later date.

Most of this work has been done with a ray tracing code which is an outgrowth of a program provided to us by Stanley Kowalski and Harald Enge of MIT.[1] Our work on program MOTER (Morris' Optimized Tracing of Enge's Rays) consists basically of the addition of an optimizer, an objective function definition, a random ray generator, and a few new elements to the MIT code. We have made several checks to prove that rays are traced identically with Kowalski's code. We assume here a familiarity with the MIT code although, to our knowledge, a report of this work has not been published elsewhere.

II. First Order

We start with the premise that first order optics and economics together dictate the basic design of any system. The principles of first order optics have been presented elsewhere[2] and a very general program, TRANSPORT,[3] is in widespread use for performing first order calculations. In designing a spectrometer, it is important that high resolution be obtained at minimum cost. In Ref. 2, an equation for first order resolving power has been derived

$$R_1 \propto_o \alpha \int_o^{\alpha_{max}} S_x(\alpha)\, d\alpha \qquad (1)$$

where $d\alpha$ is the differential bending angle and $S_x(\alpha)$ is the amplitude of the sine-like ray at location α. To minimize cost, one should minimize the weight of bending magnets. The weight of such magnets can be minimized if their width is minimized; such a condition obtains if $S_x(\alpha)$ is large and nearly constant throughout the bends.

It is not sufficient to minimize the width of the bending magnets since one must simultaneously minimize their gap height. In many cases, the y-plane mode is not strongly constrained by system performance and can be adjusted to minimize the gap of the bending magnets. For the case of an ellipsoidal phase space and a uniform field bending magnet, the minimum gap occurs if there is a waist in the center of the magnet. Near this waist, the beam size is given by the relation

$$y = y_w\left(1 + \frac{z^2 p^2}{y_w^4}\right)^{1/2} \qquad (2)$$

where y_w is the half-size of the beam at the waist, z is the distance from the waist, πp is the beam phase space $\pi y_w \phi_w$, and ϕ_w is the half-divergence of the beam at the waist. The minimum gap under these conditions is given by the relation

$$g/2 = \sqrt{L\, p} \qquad (3)$$

where L is the full length of the magnet. Note that for an H magnet the ratio of width to gap should be greater than 4:1 to minimize cost.

III. Second Order

In many cases we are concerned with minimizing the contribution of second order terms to the spot size. In a second order approximation to a system, the mean square spot size can be written

$$\langle [x_i(1)]^2 \rangle = \langle [\sum_j M_{ij}\, x_j(0) + \sum_{k\ell} T_{ik\ell}\, x_k(0)\, x_\ell(0)]^2 \rangle \qquad (4)$$

where $x_i(0)$ $[x_i(1)]$ is the i-th component of a ray vector at location 0[1] in a system. For a phase space which is upright at location 0, we find that

$$\langle [x_i(1)]^2 \rangle = \sum_j M_{ij}^2 \langle x_j^2(0) \rangle + \sum_{k\ell} T_{ik\ell}^2 \langle x_k^2(0) x_\ell^2(0) \rangle . \qquad (5)$$

*Work performed under the auspices of the U.S. Atomic Energy Commission.

Since the T_{ijk}'s are linear functions of the sextupole strengths,[2] a straightforward solution to minimizing the spot size can be obtained.

We have found that in many cases the sextupole strengths required to minimize the spot size are too large to be physically obtainable. In such cases, it may still be possible to find an acceptable solution if we minimize the quantity

$$\langle [x_i\ (1)]^2 \rangle + \frac{1}{\sigma^2} \sum_m S_m^2 \qquad (6)$$

where the S_m's are the adjustable sextupole strengths of the problem and σ is a weight which is adjusted by trial and error. By choosing σ small enough, it is always possible to obtain a solution with physically obtainable sextupoles. Of course it is possible that a system cannot be corrected, in which case only a small improvement in the mean square spot size can be obtained for reasonable sextupole strengths. We have written a special program (MINIM) to do the minimization defined above. It is possible to build such a procedure into TRANSPORT.[4] However, we feel that our program is more flexible and requires less computer time, hence we have not attempted to modify the TRANSPORT code.

If the use of the above procedure results in an unsatisfactory solution, we may try two additional remedies. The first is to use a tilted focal plane. The above technique can be used as long as the T_{ijk}'s are defined on the tilted focal plane.[4] A more powerful technique consists of measuring several components of the ray vector for each event, then letting the data acquisition computer correct for higher order terms. For example, if there is a large $\langle x|\theta^2\rangle$ term, it may be possible to measure θ well enough to correct this term by computation without using any sextupoles. A program (MINIM3) has been written to optimize sextupoles for the case when several quantities are measured, but with finite measuring errors. By using this technique and measuring x, θ, y, and ϕ, a factor of ten reduction in the second order contribution to the EPICS spectrometer resolution resulted. This improvement was required to make construction of this spectrometer feasible.

IV. High Quality Dipoles Using H_t Windings

Before going on to the extension of these procedures to ray tracing, we should pause to consider the elements available to the spectrometer designer. Dipoles form the heart of any spectrometer system and the most severe requirements for field quality usually occur in these elements. Following the suggestion of K. Halbach,[5] we have built our magnets with a series of trim windings whose purpose is to provide an adjustment of the midplane field of a dipole. In Fig. 1, we show the cross section of our prototype magnet which has seven pairs of trim windings at the interface between the pole tip and the yoke. We call these windings H_t windings, since they are designed to provide a tangential component of H at the iron/air interface. H_t is related to the midplane field by the relation

$$H_y(x,0) = \int_{-\infty}^{\infty} H_x(x',g) \tanh\left(\pi \frac{x-x'}{g}\right) \frac{dx'}{g} \qquad (7)$$

where $H_y(x,0)$ is the large (uniform) field component of the dipole. In Fig. 2, we show the field observed in the gap with no current in the H_t windings. In Fig. 3 we show the field observed after one iteration of our H_t winding adjustment program. The initial procedure for determining the appropriate adjustment for these windings is quite complicated; however, the results seem to be quite reproducible. We note that the rate at which adjustments to the main current are made severely affect the field distribution. In Fig. 4 we show the field observed after a linear change in current from 21 kG to 14 kG in two minutes. In Fig. 5 we show the field observed with the same change made over a five minute time period.[6]

We have adopted an unconventional approach to the design of the ends of the dipoles. A drawing of the version of the ends adopted for the EPICS channel is shown in Fig. 6. We used a saddle coil and a very close in field clamp to minimize the effect of the location of the coil on the effective edge. We have constructed straight coils which do not attempt to follow the effective edge since our calculations show only a small effect, and we have compensated this by a small distortion of the field clamp. We hope that any remaining effect can be corrected by an adjustment of the central field using the H_t windings. Should that be impossible, we can modify the field clamps without large additional expense. In Table I we present the calculated location of the effective edge as a function of field and as a function of nose position.

TABLE I

B_o (kG)	nose (inches outside reference)	e.f.b. (inches inside reference)
0.	2.8	.8824
0.	3.8	.6706
0.	4.8	.4915
0.	5.8	.3458
7.9	4.8	.4910
12.6	4.8	.4913
16.6	4.8	.4910
18.6	4.8	.4909

In Table II, we present the calculated coefficients[6] for the ray tracing program as a function of nose location. Also shown is the TRANSPORT input parameter k_1.[3]

We have found that it is very inexpensive to purchase large SCR power supplies with regulation between 10^{-4} and 10^{-5} depending on the quality of the current monitor used. For powering the EPICS beam line, we have purchased one 1000 kW main

TABLE II

Coefficient	nose position 2.8 in.	4.8 in.	5.8 in.
C_o	.11755	.22389	.27021
C_1	1.9592	1.6389	1.5550
C_2	-.30315	-.42538	-.43643
C_3	.62766	.39693	.33542
C_4	-.061845	-.077843	-.091894
C_5	.017904	.045927	.043207
K_1	.3924	.4626	.4920

supply and four smaller shunt supplies (-0 to -4%). All four magnets will be powered in series; the shunts will provide individual adjustment. Should the regulation of the system prove inadequate, we will later use the shunt supplies as the final stage of regulation. This whole system with transductor reference was purchased for $35/kW.

V. High Quality Quadrupoles

In a paper presented to this conference by W. Hassenzahl, it is demonstrated that it is now possible to design and build quadrupoles which have less than the order of 0.1% harmonic content in the integrated field. Such quadrupoles can be made either in a conventional symmetric form or in a narrow version without detectable loss in field quality.

VI. Detectors

Many critical assumptions about detectors are built into present-day spectrometer designs. It appears that for many applications, multi-wire proportional chambers have great promise.[7] At Los Alamos, we have developed a bifilar helical chamber which gives better than 0.33 mm fwhm resolution for minimum ionizing particles incident normal to the chamber (see Figs. 7 and 8) and can handle a maximum instantaneous rate approaching 10^6 particles/second.[8] A simpler version of this chamber is presently under development. This simpler version has been used with 15 MeV protons incident at 55° to the normal. We observed 0.6 mm fwhm resolution in this test; all of this width could be explained by the beam size so that a good measurement of the resolution has yet to be made.[9] We expect to be able to achieve 0.25 mm resolution with both versions of helical chambers. For heavy ion work, it is likely that such chambers can give as good dE/dx and timing information as is available from any proportional chamber.

In order to use these chambers with spectrometers, it is necessary to be aware of their limitations. First, it is difficult to make a chamber more than 0.5 m long. Second, it is likely that resolution degrades seriously if the chambers are not normal to the beam and minimum ionizing particles are detected (in high energy applications, spark chamber resolution degrades on the order of a factor of two for particles incident at 45° to the normal). For high and medium energy applications, it is possible to use two detectors to project to the focal plane without serious loss of resolution since multiple scattering can be small. Finally, proportional chambers cannot easily be made to conform to a curved focal "plane," particularly one that is curved in two dimensions.

VII. Program MOTER

Modifications to Ray Tracing

We have made several modifications to the basic ray tracing. First, we changed the method of integration to the "predictor corrector" method. In addition, a helix is used in the uniform field region of dipoles. Since the magnetic field is evaluated less than half as often, a factor of two improvement in running time was expected. The new code is significantly faster, but the expected improvement was not observed.

In the fringe field region of dipoles we now use revised formulas to derive the midplane field. The midplane field is given by the expression

$$B_y = \frac{B_o}{1 + \exp(C(S))} \tag{8}$$

and

$$C(S) = C_o + C_1\, S + C_2\, S^2 + C_3\, S^3 + C_4\, S^4 + C_5\, S^5. \tag{9}$$

In our version of the program, gS is the distance from the point of field evaluation to the effective edge, and g is the full gap of the dipole. S is determined numerically. In order to speed up the calculation, we changed the basic second order shape from a circle to a parabola. At the same time, we normalized the higher order terms as shown in the equation for the effective edge below:

$$-Z = \mathrm{RAP}\left(\frac{x}{RW}^2\right) + \mathrm{CAT}\left(\frac{x}{RW}^3\right) + \mathrm{CFV}\left(\frac{x}{RW}^4\right) + \mathrm{CNN}\left(\frac{x}{RW}^5\right). \tag{10}$$

The quantity RW is usually chosen to be the first order beam size plus one gap. The new definition of the coefficients is such that for coefficients of equal magnitude, the effect of each order on the outermost rays is approximately the same.

We have changed the quadrupole subroutine to the improved version, POLES, provided by S. Kowalski.[10] This subroutine allows for all multipoles through duodecapole in the interior region. Expansion of the quadrupole field is accurate through fifth order in the fringe field region. However, there is a fundamental problem of obtaining input data for this code. In the region where there is a variation of the field with z, the field due to the quadrupole can be expanded in the form

$$H_r(z,\theta) = \left(\sum_{n=1}^{\infty} A_{2n}(z)\ r^{2n-1}\right) \sin 2\theta. \qquad (11)$$

Rotating coil measurements with a short coil are related to the sum of all terms; the program POLES uses $A_{21}(Z)$ as input.[11] We at Los Alamos have not yet found time to determine A_{21} from the data. We know of no published work on this problem. More serious difficulties exist for the higher harmonics since for good magnets they are zero except in the fringe field region.

We have added new elements to the ray tracing package which perform the following functions: DRIFT; SLIT, which includes multiple scattering and energy loss for a wedge absorber; SEPARATOR, which simulates the crossed field separator used in the EPICS beam; and FOCAL, which provides for a tilted, curved focal "plane." These elements are required for ray tracing of all the beams and spectrometers at Los Alamos.

Definition of Figure-of-Merit

The first and most important step in automatic optimization of parameters was the definition of the figure-of-merit. We chose a generalized mean square resolution since it is a compromise between the full width at half-maximum and the full width at the base which are commonly used as a measure of spectrometer resolution. In addition, this definition offers simplicity of calculation and allows us to choose from a large number of optimization programs available for use with the least squares problem. Finally, this figure-of-merit is directly applicable to on-line ray tracing using particle beams.

We minimize the following quantity

$$\Phi = \sum_{i=1}^{\alpha} \frac{D_i}{\sigma_i^2} + \sum_{j=1}^{\beta} \frac{S_j^3}{\sigma_j^2}\ . \qquad (12)$$

In the above expression, the σ's are arbitrary weights to be adjusted by the user. The D terms ("Demands") each have the following form

$$D_i = \left\langle \left(\sum_{k=1}^{\gamma} c_{ik}\ P_k\right)^2 \right\rangle\ . \qquad (13)$$

The brackets indicate an average over the phase space of the beam. The P_k's are products of up to four terms of the form

$$X_{comp1}(Loc_1) \cdot X_{comp2}(Loc_2) \cdot \cdot X_{comp4}(Loc_4). \qquad (14)$$

Each of these indicates one of the six components of the vector defining a ray at a particular location in a beam. The c's are either fixed or adjusted as part of the optimization (but at least one of the c's in each demand must be fixed in order to have a well defined objective function Φ).

The S ("strength") terms are put in as a penalty for large multipole strengths in an analogous way to the penalty applied for large sextupole strengths in the second order program discussed earlier.

A few examples may increase the clarity of the demand definition. In these examples, location 0 is the entrance to a system, location 1 is the exit of a system, and the six components of the ray vector are x, x', y, y', L, δ in the notation of the TRANSPORT program.

A demand appropriate for a simple spectrometer is

$$\langle [x_6(0) + c\ x_1(1)]^2 \rangle \qquad (15)$$

where c is adjustable. Minimizing this expression will optimize the resolution, and the best fit value of c is the negative of the dispersion. To make an image with a magnification of -1, one would minimize

$$\langle [x_1(0) + x_1(1)]^2 \rangle\ . \qquad (16)$$

If we want to design a spectrometer with a position sensitive detector at the entrance and a position and angle sensitive detector at the exit, and in addition we want to assume that the data analysis program is to correct for a large $\langle x|x^2\rangle$ aberration in the forward direction and a large $\langle x|\theta^2\rangle$ aberration in the backward direction, we would minimize the expression

$$\langle [x_6(0)+c_1x_1(0)+c_2x_1(1)+c_3x_1(0)x_1(0)+c_4x_2(1)x_2(1)]^2 \rangle. \qquad (17)$$

To simulate the effects of measuring errors, we simply substitute $\tilde{x}$ for x everywhere in the demand, where

$$\tilde{x} = x + \varepsilon \qquad (18)$$

and ε is a small random measuring error. When measuring errors are included, the brackets indicate an average over the phase space of the beam and a large number of measurements.

Optimizer

We use an optimizer based on a modified version of the Levenberg Method[12] which has been used for optics problems at Los Alamos for many years. The required derivatives are obtained numerically. This method is particularly suited to problems such as this in which calculation of derivatives is expensive in computer time whereas calculation of Φ is less expensive. Note also that the normalization of the effective edge parameters chosen earlier allows a single step size for numerical differentiation which can be used for parameters of all orders. In addition, the derivative matrix is better conditioned than would have been the case with the MIT definitions.

Random Ray Generator

In some cases, it is necessary to consider beams which have large phase space in five dimensions. We have found that a reliable calculation of the resolution can be obtained with far fewer rays if we use randomly chosen rays rather than a ray set with uniform spacing. For example, to accurately define all terms through fifth order in a system with midplane symmetry, 1875 rays would be required. On the other hand, with 15 adjustable parameters, we have found that 50-100 randomly chosen rays are sufficient for the optimization.

The modifications to the ray tracing code required to use random rays include inserting a ray generator and a method of simulating the apertures of the system. In addition, several changes were required to prevent rays from using a large amount of computer time if they enter an undefined region of magnetic field. With the random ray generator and the simulated apertures, we believe that reliable calculation of the acceptance of a system is possible. At present, we are limited to 400 rays, or 5% statistical accuracy.

VIII. Applications

HRS Beam Line

The 800 MeV high resolution proton spectrometer (HRS) system at Los Alamos consists of two parts; a beam line made of five bending magnets and 12 quadrupoles, and a spectrometer consisting of two bending magnets and one quadrupole (Fig. 9). The beam line provides a dispersed beam with adjustable vertical dispersion. In the horizontal plane a small, parallel beam is required which is approximately independent of the dispersion adjustment. The design resolution of the beam line is 1 part in 10^5.

The beam line consists of three sections: first, a 6^o deflection system to separate the H^+ and H^- beams; second, two horizontal 57^o bending magnets to provide the required dispersion; and third, a ten quadrupole system which twists the dispersion to the vertical plane and provides for adjustable dispersion. The first order design was done with TRANSPORT. Second order difficulties occurred only for chromatic aberrations; it was possible to correct only the $\langle y|\theta\delta\rangle$ term. Using program MINIM, we optimized the four radii on the 57^o magnets to simultaneously optimize the resolution over the whole range of dispersion adjustment (from 15 cm/% to 66 cm/%). Then using MOTER, we adjusted the quadrupoles to give correct first order properties. The resulting resolution was close enough to specifications that no higher order corrections were required. The resulting resolution function is shown in Fig. 10. We also tried changing from the early quadrupole subroutine to POLES and saw no observable change in the resolution.

QDD Spectrometer

The HRS spectrometer is a QDD which was designed by Kowalski and Enge[12] before MOTER was written (Fig. 11). The focal plane angle was to be 30^o; we planned to use detectors normal to the central ray and project to the focal plane. The high order corrections required are small and only second order corrections were built into the pole tips. J. Spencer recently designed the field clamps using the MOTER program. The calculated resolution using detectors normal to the beam was approximately 10^{-4}. Putting in all the information available at the exit of the spectrometer reduced this a factor of four. An additional factor of two was obtained by using MOTER to optimize the field clamps on the four magnet boundaries. The resolution function for $\pm$ 2.5% momentum spread before and after the MOTER adjustment is given in Fig. 12. Note that by optimizing mean square resolution, we simultaneously improve the full width at half-maximum and the full width at the base.

EPICS Beam Line

The Energetic Pion Beam and Spectrometer System (EPICS) is a high resolution system designed for pion scattering experiments between 100 MeV and 300 MeV. The beam line consists of four bending magnets and a crossed field separator (Fig. 13). In this system, all eight magnet edges have fourth order curves to correct aberrations.

The original design goal was for 10^{-4} resolution and a focal plane normal to the central ray. The system was first designed with TRANSPORT. The program MINIM was used to correct second order aberrations. A search of first order parameter space was required to find a design which could be corrected with reasonable edge curves. In this search, more than 90 different first order designs were considered. The resulting second order design indicated that 10^{-4} resolution could be achieved.

Ray tracing this system with MOTER proved to be quite troublesome. It is difficult to generalize from the experience and our best guess as to what happened is that the second order corrections required were very strong, increasing the troubles with higher order aberrations. The optimized solutions with MOTER always reduced the second order strengths and put in some higher order curves as well. In the end, we settled for 2.4×10^{-4} resolution for a system with a normal focal plane, a solid angle of 3.5 msr, and a momentum acceptance of 2%. The resolution function for the EPICS beam is shown in Fig. 14. Note that without the MOTER program, it would have been impossible to build this beam line.

EPICS Spectrometer

The spectrometer for EPICS was the most difficult design problem of all those we faced at Los Alamos. The major new features we had to cope with were the large target size (20 cm x 10 cm), the large momentum spread ($\pm$ 10%), and the length

requirement imposed by the short lifetime of the pion. The final design, which M. Thomason and H. Thiessen came up with, consists of a symmetric triplet which images the target onto the first detector. A DD spectrometer is then used to measure the scattered particle momentum (Fig. 15). This EPICS system is an "absolute" system in the sense that both the beam particle momentum and the scattered particle momentum are measured; in the HRS and some other systems, only the difference between these momenta are measured.

The bending magnet apertures are very close to the minimum required to transport the phase space through the bends. This was accomplished by simultaneously adjusting the focal length of the triplet and the edge angles of the bends to give the required y waist size at a location midway between the bends. Second order calculations using MINIM3 indicated that 10^{-4} resolution could be achieved. Before deciding on this design, we tried second order calculations on many systems and observed a correlation between cheaper systems and better resolution in second order.

When we ray traced this system with MOTER, we had even more difficulty than with the channel. To investigate what the source of the difficulty was, we fit all 70 coefficients through fourth order to a set of 400 rays. Then we remove some of the smaller terms to see the relationship between the number of terms and the resolution. We also calculated the resolution for several different sets of measuring errors. The results are shown in Fig. 16. A resolution function is shown in Fig. 17. These results are somewhat obsolete, since we have recently found a set of 19 terms which gives only slightly worse resolution than the 33 terms used for Fig. 17. We decided to build this system since it approximately matches the beam and no better system was available. If we did not have the full power of all the features built into MOTER, it would not have been possible to have confidence that the spectrometer would work properly.

Other Applications

In collaboration with Ole Hansen and E. Flynn, we have tried redesigning the QDDD with MOTER and found that it is possible to make a factor of two improvement in the resolution by varying a few parameters. Perhaps a further improvement is possible, however this is an academic exercise since the LASL QDDD is already on order and it is too late to change the drawings. Perhaps it would be reasonable to consider redesigning the field clamps at a later date.

Two other systems similar to the EPICS spectrometer are presently being studied in Europe. At SIN, there is a proposal for a pion beam and spectrometer designed to compete with EPICS which uses several planes of detectors to keep the aberrations under control.[14] There is also a proposal for a beam and spectrometer for studying hypernuclei at the CERN PS.[15] Both of these groups will need to perform an analysis of their resolution which is similar to ours to have confidence that these systems will work.

IX. Conclusion

We have made several important improvements in the technology of ray tracing which allow us to design a wide range of magnetic optical systems with confidence. These techniques bridge the gap between low energy work in which multiple scattering is dominant and requires a well-defined focal plane, and high energy work in which it is possible to use a large, poor quality magnet and reconstruct momenta by using a sufficient number of measurements. The technique of using as much information as is available for each particle together with a well-designed spectrometer shows great promise for making possible cheaper and better systems in medium energy and high energy applications.

X. Acknowledgements

We gratefully acknowledge many hours of discussions with Klaus Halbach, Karl Brown, and Harald Enge, and the many useful ideas which were developed therein. N. Tanaka, J. Spencer, M. Thomason, R. Stearns, and R. Rolfe performed the measurements and analysis of the prototype magnet. We wish to thank K. Halbach, David Lee, Ole Hansen, and E. Flynn for permission to report highlights of their work prior to publication. Ron Yourd performed all the field calculations.

XI. References

1. S. Kowalski and H. Enge, private communication.
2. Karl L. Brown, "A First- and Second-Order Matrix Theory for the Design of Beam Transport Systems and Charged Particle Spectrometers," Advances in Particle Physics 1, 71 (1968).
3. Karl L. Brown and S. K. Howry, TRANSPORT/360, SLAC 91 (1970).
4. David Carey, NAL, private communication.
5. Klaus Halbach, Nuclear Instruments and Methods (to be published).
6. Further details of this work can be found in a paper submitted to this conference by W. Dunwoody, et al.
7. G. Charpak, Ann. Rev. Nucl. Sci. 20, 195 (1970).
8. D. Lee, S. Sobottka, and H. A. Thiessen, Nuclear Instruments and Methods (to be published).
9. D. Lee, private communication.
10. S. Kowalski, private communication.
11. We are grateful to K. Halbach for pointing out this difficulty.
12. T. Doyle, LASL, private communication.
13. H. Enge, Deuteron Inc., private communication.
14. R. Frosch, SIN, private communication.
15. V. Lynen, CERN, private communication.

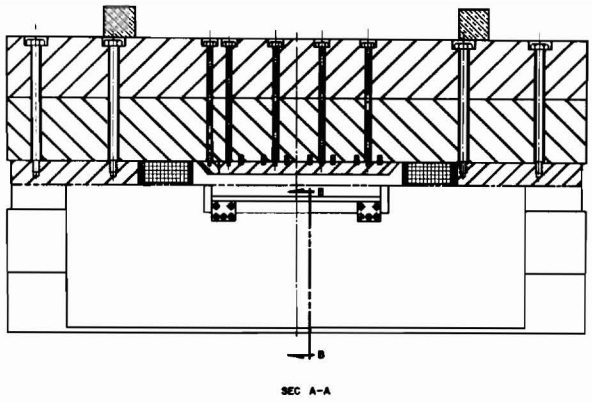

Fig. 1. Cross section of prototype magnet with H_t windings.

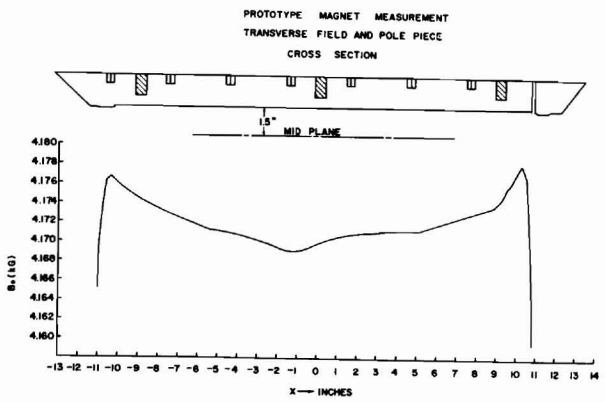

Fig. 2. Midplane field in prototype magnet with no excitation of H_t windings.

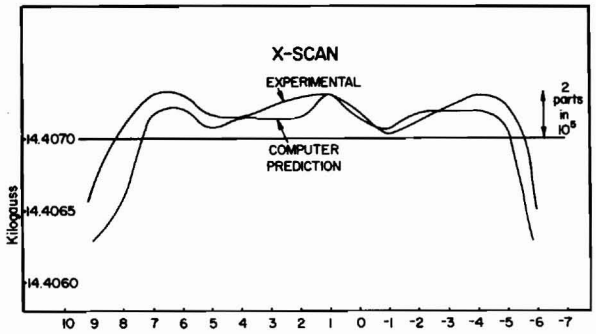

Fig. 3. Measured midplane field of prototype magnet compared with the computer prediction for optimized H_t winding currents.

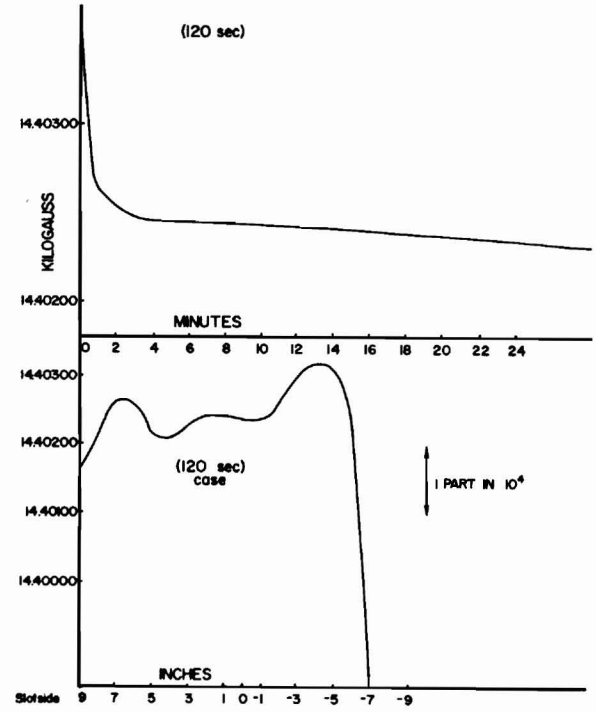

Fig. 4. Measured midplane field of prototype magnet after a two minute change in field from saturation to 14 kG.

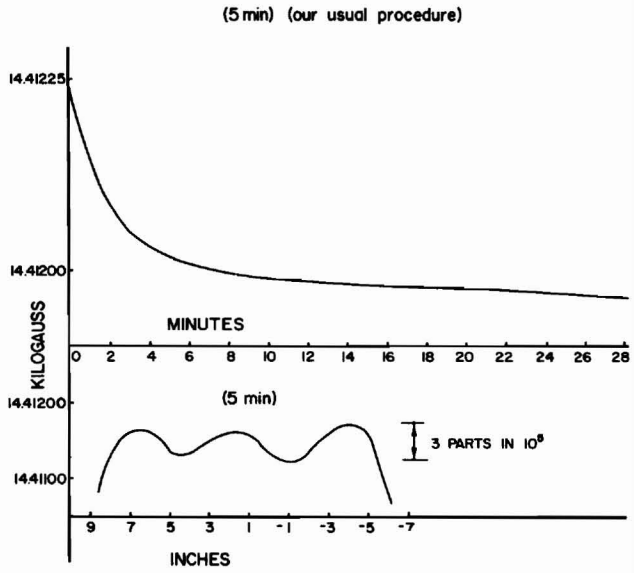

Fig. 5. Measured midplane field of prototype magnet after a five minute change in field from saturation to 14 kG.

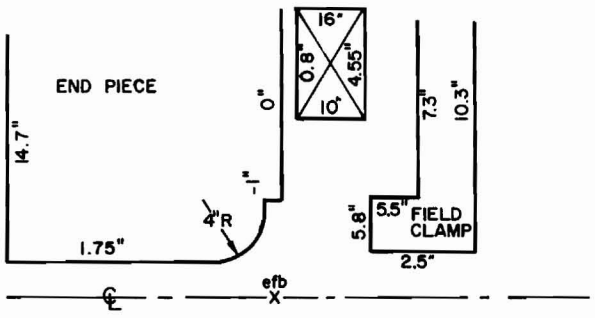

Fig. 6. End geometry for EPICS dipoles.

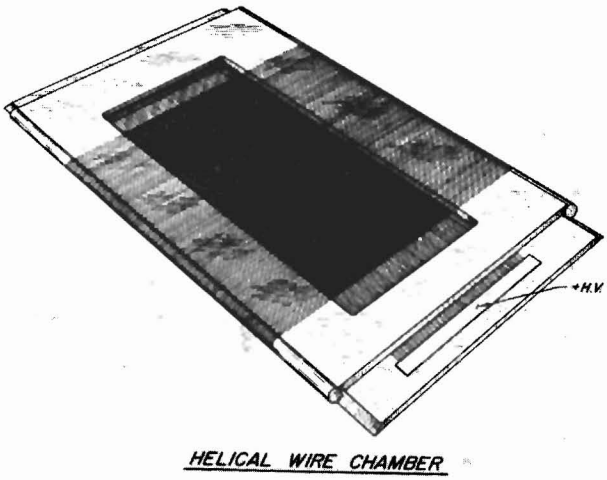

Fig. 7. Helical multiwire proportional chamber.

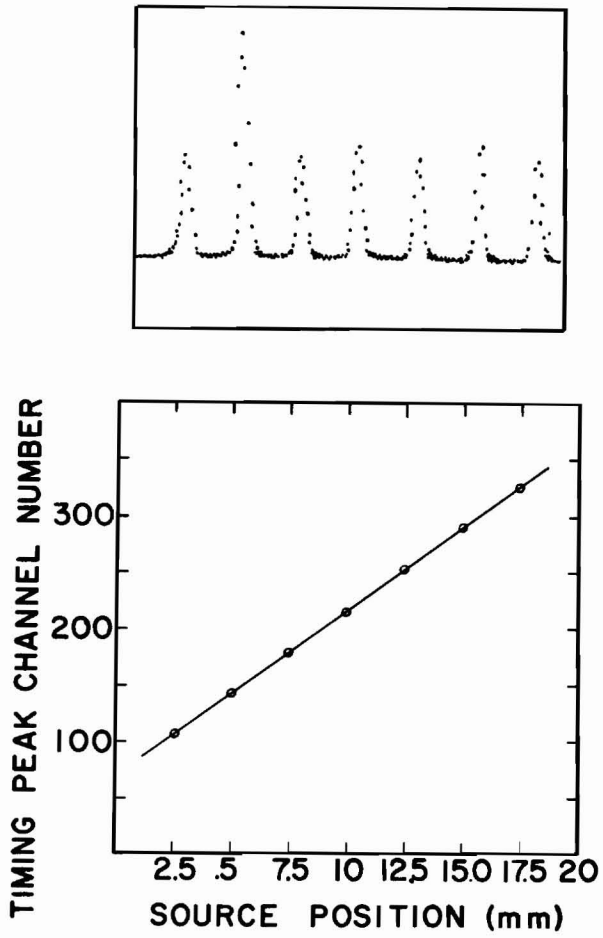

Fig. 8. Resolution and linearity of bifilar helical chamber.

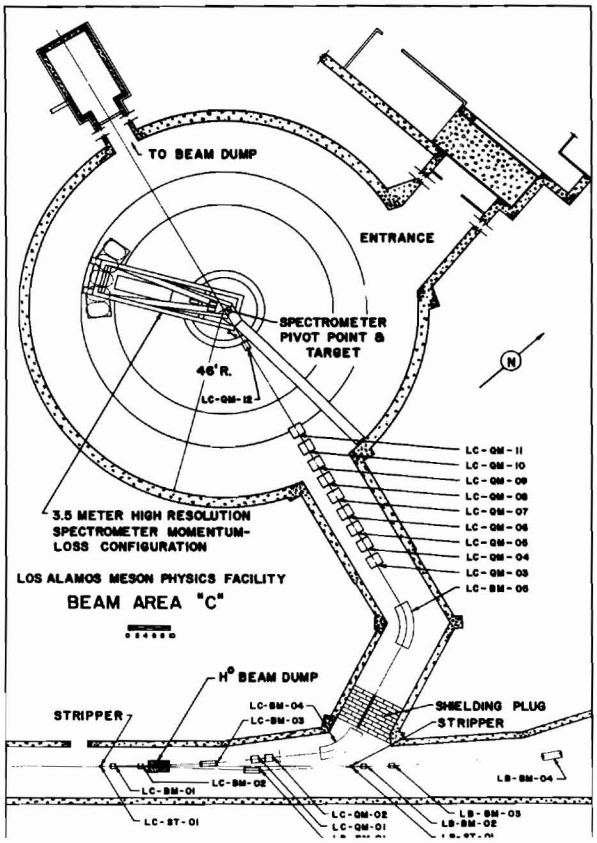

Fig. 9. Plan view of HRS beam line.

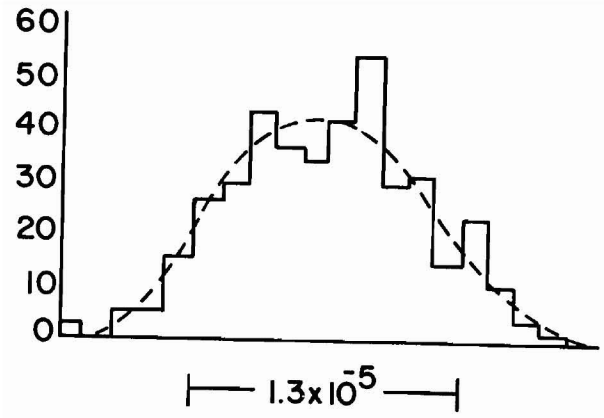

Fig. 10. HRS beam line resolution function.

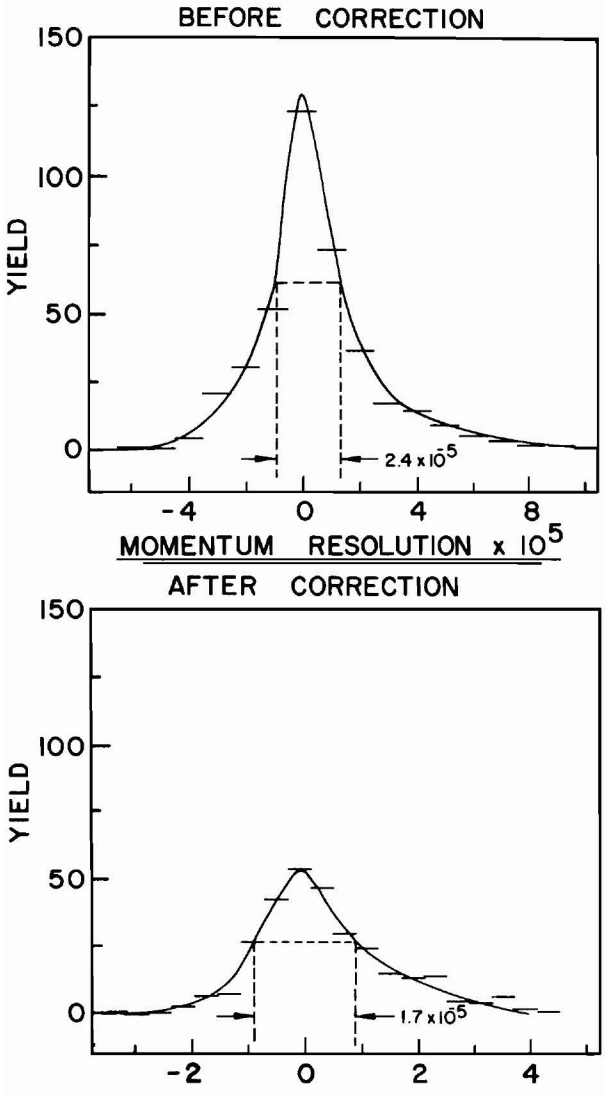

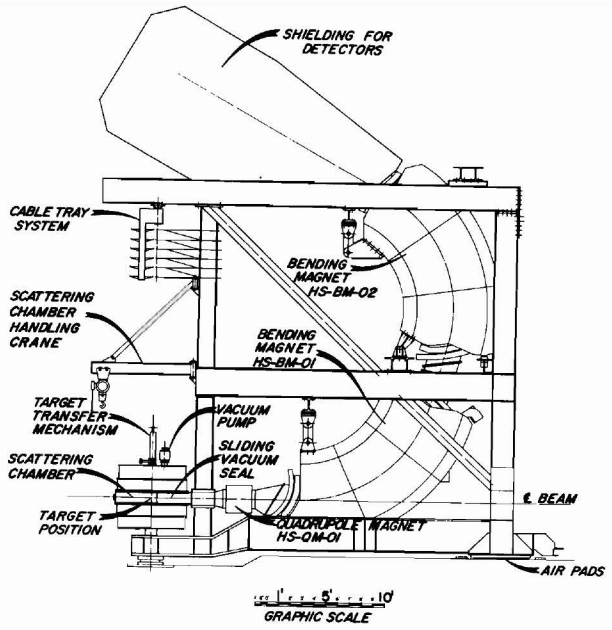

Fig. 11. HRS spectrometer, elevation view.

Fig. 12. HRS spectrometer resolution function before and after optimization of the field clamps.

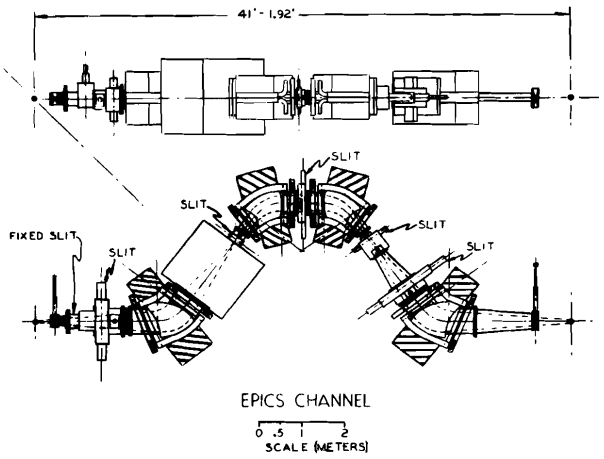

Fig. 13. EPICS beam line, elevation view.

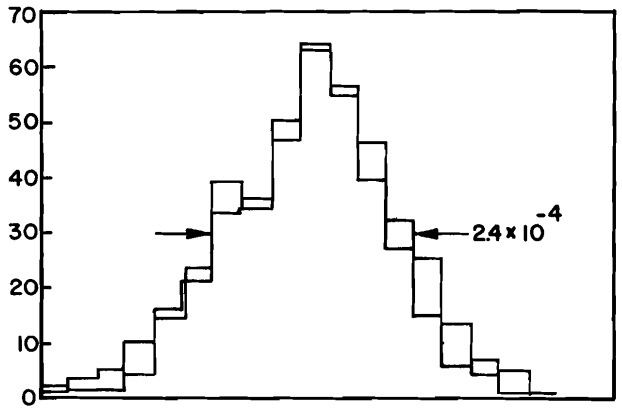

Fig. 14. EPICS beam line resolution function

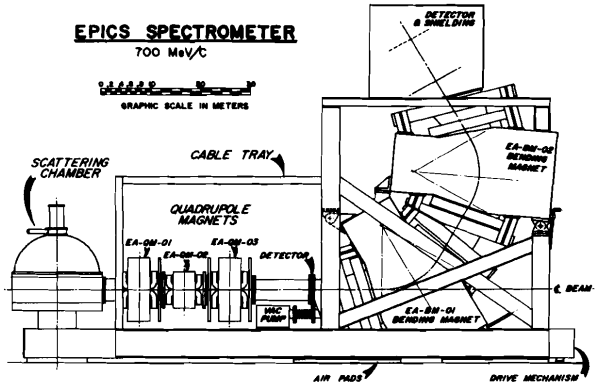

Fig. 15. EPICS spectrometer, elevation view.

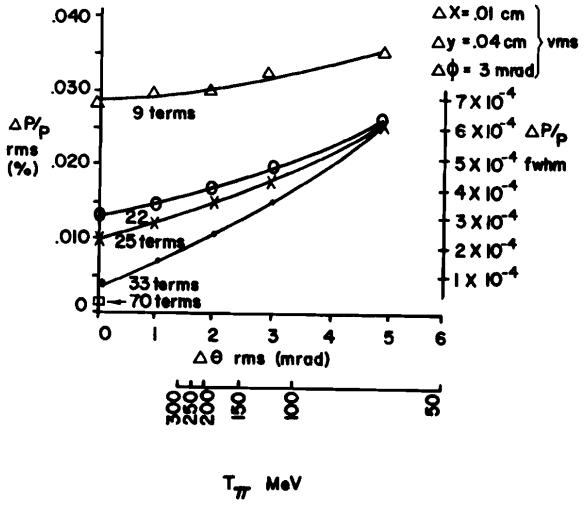

Fig. 16. EPICS spectrometer resolution vs number of terms and energy.

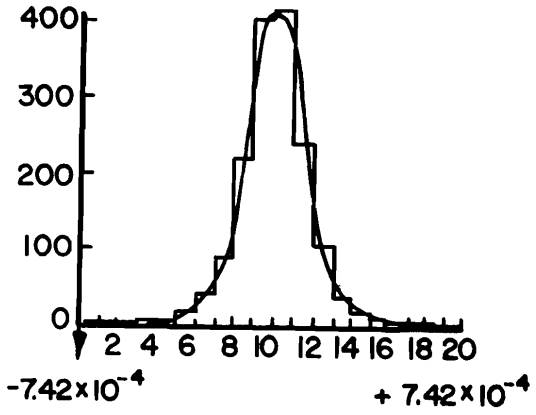

Fig. 17. EPICS spectrometer resolution function.